Journal of Cluster Science (2022) 33:413–420
https://doi.org/10.1007/s10876-021-01978-w

ORIGINAL PAPER

A Facile Approach Based on Functionalized Silver Nanoparticles as a Chemosensor for the Detection of Paraquat

Shujat Ali[1] · Muhammad Raza Shah[2] · Sajid Hussain[3] · Sikandar Khan[3] · Abdul Latif[3] · Manzoor Ahmad[3] · Mumtaz Ali[3]

Received: 11 August 2020 / Accepted: 22 December 2020 / Published online: 22 January 2021

Abstract

In this study, a simple approach was developed based on imidacloprid stabilized silver nanoparticle (Imida-AgNPs) for the sensitive detection of paraquat pesticide. Experimental parameters were optimized for the synthesis of the proposed sensor. Imida-AgNPs, synthesized under the optimized reaction condition were characterized by UV–Vis spectrophotometer, Fourier transform infrared (FT-IR) spectroscopy and atomic force microscopy (AFM). The Imida-AgNPs were spherical in shape with an average size of 40–70 nm. The stability of Imida-AgNPs was checked towards changes in temperature, time, pH, and salinity. The synthesized Imida-AgNPs were tested as a colorimetric sensor to detect a trace amount of paraquat for the first time. The developed sensor was green, simple, selective and economical. The calibration curve for detection of paraquat was found linear over the concentration range of 20–180 μM. The standard deviation (SD) was found to be 0.0019 μM with relative standard deviation (RSD) of 0.027%. The limit of detection (LOD) and limit of quantification (LOQ) were found to be 6.27 μM and 19 μM respectively. Importantly, the sensor was successfully employed for the detection of paraquat in real samples.

Keywords Silver nanoparticles · Pesticide · Imidacloprid · Nanosensor · Paraquat dichloride

Introduction

Paraquat (1,1-dimethyl-4,4-dipyridinium chloride) is widely used as a quaternary ammonium herbicide all over the world due to its low cost and remarkable effects on plant cells for crop protection as well as horticultural use [1]. Its herbicidal properties were first discovered in 1955 and it was introduced commercially in 1962 [2]. Paraquat kills plants rapidly by deactivating the photosynthetic mechanism due to their redox potential. Paraquat ion binds near the ferrodoxin (FRD) binding site in photosystem I (PSI), and accepts an electron, becoming paraquat monocation free radical (PQ^+), which initiates a series of reactions leading to cell membrane disruption and plant death [2]. However, it is extremely toxic to both animals and humans, leading to thousands of fatalities and hospital admissions due to accidental or intentional pesticide poisoning, especially in non-developed countries [3]. The estimated oral lethal dose (LD_{50}) of paraquat in humans is 35 mg/kg (20% solution 10–15 ml). The oral LD_{50} value for monkeys is 50 mg/kg, for rats is 110 to 150 mg/kg and for cows is 50 to 70 mg/kg [4]. It causes cellular damage and necrosis in the brain, heart, lungs, liver, and kidneys. As a result, due to its high acute toxicity and lacking a specific, effective antidote [1], it has been banned for sale and uses in many countries in recent years [5]. In this connection, the development of efficient techniques for the detection of paraquat has great significance. Hence, several analytical methods have been reported for the detection of paraquat such as flow injection analysis [6], gas chromatography [7], liquid chromatography [8], thin-layer chromatography [9], electrophoresis [10], mass

✉ Mumtaz Ali
mumtazphd@gmail.com

[1] School of Food and Biological Engineering, Jiangsu University, Zhenjiang 212013, People's Republic of China

[2] H.E.J. Research Institute of Chemistry, International Center for Chemical and Biological Sciences, University of Karachi, Karachi 75270, Pakistan

[3] Department of Chemistry, University of Malakand, Khyber Pakhtunkhwa 18800, Pakistan

spectrophotometry [11], and electrochemistry [12]. Although these techniques can be efficiently used for pesticide detection with high selectivity and sensitivity, but these methods are expensive, time-consuming and complicated in operation [13]. Therefore cheap, sensitive, robust, selective, and technically simple yet effective methods for detection of paraquat are still needed. In contrast to these techniques, colorimetric detection is the most convenient analytical technique in analyzing various biological samples because of its inherent simplicity, high versatility and sensitivity [14, 15]. Therefore, efforts have been made to synthesize low cost and user-friendly chemosensors for many years [16].

Currently, silver nanoparticles (AgNPs) have gained enormous popularity in the field of sensors due to their significant chemical, optical and electronic properties [17, 18]. The AgNPs offer high surface energy that promotes surface reactivity. Spectral properties of AgNPs depend entirely on their size, shape, inter-particle spacing and environment [19, 20]. Therefore, the geometry of these nanoparticles would provide significant control over linear and nonlinear optical properties [21]. These properties allow AgNPs to be used in various chemical and biological sensing applications such as a colorimetric sensor for histidine [22], real-time probing of membrane transport in living microbial cells [23], enhanced Infrared (IR) absorption spectroscopy [24], laser desorption/ionization mass spectrometry of peptides [25], colorimetric sensors for measuring ammonia concentration [26], glucose sensor for medical diagnostics [27], an optical sensor for hydrogen peroxide [28] and biosensors for detection of pesticides [29].

Imidacloprid (1-[(6-chloro-3-pyridinyl) methyl]-N-nitro-2-imidazolidinmine) is a widely used insecticide in agriculture. It was synthesized in 1985 by Nihon Bayer Agrochem. Imidacloprid (Imid) is highly effective against sucking insects like aphids, whitefly, leafhoppers and mealybugs. It is also highly effective against some biting insects, including Colorado beetle and paddy stem borers. Imidacloprid is more toxic to insects as compare to mammals because it binds much more strongly to insect neuron receptors than to mammal neuron receptors [30, 31]. Imidacloprid was chosen for this work because of its little chronic effect on mammals and their strong interaction with silver ion due to the electron-donating ability of nitrogen atoms of Imidacloprid to silver ions.

In this article, we have synthesized imidacloprid stabilized silver nanoparticle (Imida-AgNPs) in an aqueous medium under room temperature through the chemical reduction method. The formation of synthesized nanoparticles was confirmed by UV–Vis Spectrophotometer, Fourier Transform Infrared (FT-IR) spectroscopy and Atomic Force Microscopy (AFM). The Imida-AgNPs were applied for the detection of paraquat in water and soil samples.

Experimental

Materials and Reagents

Highly pure analytical grade chemicals and reagents were used in this study such as silver nitrate ($AgNO_3$) and sodium borohydride ($NaBH_4$) were purchased from Sigma Aldrich, USA. Deionized (DI) water was provided by the industrial analytical center University of Karachi. Imidacloprid, acetamiprid, penoxyprop-p-ethyl, emamictin benzoate, cypermethrine, thiamethxion, lambda cyhalothrine, prochloraz, acetochlor chloropyrifos, pendimethalin, and paraquat were purchased from a local supermarket.

Instrumentation

The synthesized Imida-AgNPs were characterized with the help of a UV–Visible spectrophotometer (Thermo Scientific Evolution 300). The formation of nanoparticle was monitored with UV–Vis spectra in the term of the Surface Plasmon Response (SPR) band. The formation of nanoparticles was further confirmed with the help of FT-IR spectra in the dried sample using KBr disc. The FT-IR spectra were recorded between 4000 and 400 cm^{-1} on (Bruker Victor 22 spectrometer). The shape and size were measured with the help of AFM (Agilent Technology 5500 USA). A drop from the Imid-AgNPs suspension was taken, transferred on to a cleaned mica surface, dried and analyzed. For imaging, a high-frequency Si cantilever (125 μm, 22 N/m and 330 kHz) was used [32].

Synthesis of Imida-AgNPs

Imida-AgNPs with an average diameter of 40–70 nm were synthesized according to a previously reported method with slight modifications [33]. In detail, stock solutions of silver nitrate (1.0 mM) and imidacloprid (1.0 mM) were prepared and diluted to (0.1 mM). Solution of imidacloprid (0.1 mM) were mixed with (0.1 mM) of silver nitrate solution in the ratios of 5:1, 15:1,6:1,10:1, 8:1,3:1 and 1:1 in different vials. Followed by stirring and then (0.3 ml, 4 mM) solution of a freshly prepared $NaBH_4$ was added. The transparent colorless solution was immediately turned greenish-yellow which confirmed the formation of Imida-AgNPs.

Stability of Imida-AgNPs

The stability of Imida-AgNPs was checked towards changes in temperature, time, pH, and salinity with the help of

UV–Visible spectrophotometer [34]. To examine heat stability, the solution of synthesized nanoparticle was heated up to 100 °C. The stability of Imida-AgNPs in an aqueous medium of different pH (1–12) was tested with the help of pH adjustment of the colloidal solution with NaOH or HCl (0.1 M). The effect of sodium chloride (NaCl) solution on the stability of Imida-AgNPs was analyzed in the range of (0.1 mM–2.0 M). The stability of Imida-AgNPs with respect to time was also determined from initial synthesis till months to study the storage capacity.

UV–Visible Analysis and Colorimetric Detection

The chemosensing ability of imida-AgNPs was investigated toward different available pesticides (i.e acetamiprid, penoxyprop-p-ethyl, emamictin benzoate, cypermethrine, thiamethxion, lambda cyhalothrine, prochloraz, acetochlor chloropyrifos, pendimethalin, and paraquat). Pesticides solutions (0.1 mM) were prepared in deionized (DI) water and 1.5 ml of each pesticide solution was mixed with 1.5 ml of imida-AgNPs respectively. No significant color changes were observed in the solution except for the paraquat, which turned to light pink from greenish-yellow. The change in color and absorbance was determined as a measure of colorimetric sensing of paraquat. The primary interaction was checked through a UV–Visible spectrophotometer. The sensing selectivity of Imida-AgNPs towards the pesticide (paraquat) was further studied by interacting the fixed concentration and volume of Imida-AgNPs with already sensed pesticide (paraquat) and interfering pesticides (the other tested pesticides) as mentioned earlier. Further, the effects of pH (4–12), temperature (< 100 °C) and salinity were also checked using UV–Vis spectroscopy. After finding out the sensitivity and selectivity, the various concentrations of paraquat solutions were prepared and all of these concentrations were treated with an equal volume of Imida-AgNPs to trace the lower detection limits (LDL) and higher detection limits (HDL).

Real Sample Analysis

To find out the applicability of the synthesized nanoparticle for practical application, the known amount of paraquat was spiked in water and soil samples. Water was collected from the university campus. The soil sample was collected from local fields in District Swat of Pakistan. The soil was diluted ten times in DI water before use.

Results and Discussion

Synthesis and Characterization of Imida-AgNPs

Imida-AgNPs were synthesized by chemical reduction of silver ions in the presence of imidacloprid as a capping agent due to its excellent binding sites. The schematic representation of Imida-AgNPs formation is given in Fig. 1.

The strong interaction between imidacloprid and silver ions has been explained by the electron-donating ability of nitrogen atom to silver ions. The greenish-yellow color of Imida-AgNPs exhibited an absorption peak in the area of 380–450 nm (Fig. 2a) which is being the characteristic peak for AgNPs. Different molar ratios showed the absorption spectra in the area of 380–450 nm, however, the molar ratio 5:1 of $AgNO_3$ and pesticide (Imidacloprid) showed the optimum results as confirmed by UV–Visible spectroscopy (Fig. 2b). Hence, 5:1 was selected as the optimized ratio for the maximum production of the Imida-AgNPs. To confirm the interaction of Imidacloprid and silver we studied the FT-IR spectra of pure Imidacloprid and Imida-AgNPs [35]. The Imidacloprid alone exhibited peaks at 1110.50 cm^{-1}, 1140.92 cm^{-1}, 1370.12 cm^{-1}, 1410.78 cm^{-1}, 1561.78 cm^{-1} and 3347.85 cm^{-1}. The peak due to NH at 3347.85 cm^{-1} became broad which confirmed that the NH group was involved in the reduction of silver ions and stabilization of Imida-AgNPs [33] (Fig. 2c). The size and surface morphology were analyzed by AFM, the Imida-AgNPs were spherical in shape with an average size of 40–70 nm (Fig. 2d, e).

Stability of Imida-AgNPs

The shelf life and stability of freshly synthesized Imida-AgNPs was checked through physical/chemical parameters to assess their applicability in different fields [36]. Imida-AgNPs were found stable at room temperature for several days showing no aggregation or sedimentation of nanoparticles as reflected from the SPR band having no prominent change in the absorbance and wavelength (Fig. 3a). However, a slight decrease in the intensities of the peaks was observed which may be due to the diffusion of the stabilizing molecules from the NPs surfaces and subsequent changes in the shape and size of the NPs. In the same way, the synthesized nanoparticles also showed adequate stability at high temperatures, but a small decrease can be observed in SPR bands (Fig. 3b). The relatively slight decrease in the peak intensity could be attributed to the oxidative damage at high temperature [37]. However, the nanoparticles were stable and no aggregation and precipitation were observed. Similarly, the SPR bands

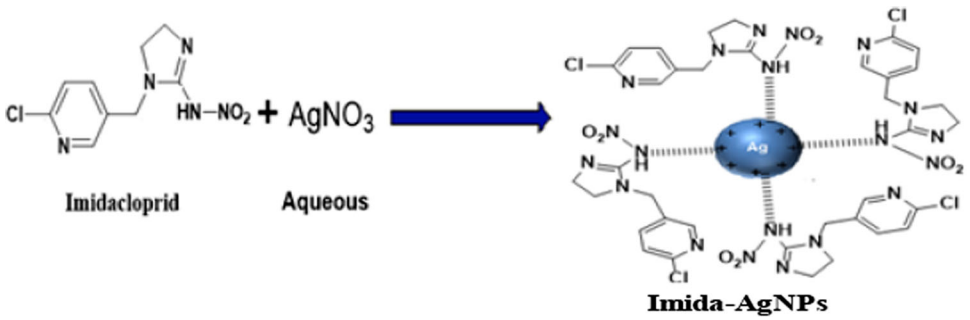

Fig. 1 Schematic representation of Imida-AgNPs formation

of Imid-AgNPs were recorded at different pH mediums (1–12). The Imid-AgNPs remain stable in the range of pH (5–10) but in highly acidic (pH < 5) and basic medium (pH > 10) reduction or distortion in SPR bands was observed (Fig. 3c). This may be due to the fact that the surface charge (that keep the NPs dispersed in solution and regulate electrostatic repulsion) of the NPs was altered in highly acidic and basic medium and resulted in little aggregation of the NPS [38]. The stability of Imida-AgNPs was checked in different concentrations (0.1 mM–2.0 M) of NaCl solution. Generally, AgNPs are not chemically stable and react strongly with inorganic ligands such as chloride (Cl^{-1}). Cl^{-1} has a strong affinity for oxidized silver and is often present in natural water and soil, hence, NaCl was used in this study [39]. As shown in Fig. 3d, an increase in NaCl concentration induced a reduction in SPR bands of Imida-AgNPs, which indicated the strong affinity of Cl^{-} for Ag^{+} ions [40].

Detection of Pesticides

Generally, the interaction of conjugates with nanoparticles may detect either by quenching or shifting of SPR band. Imida-AgNPs was investigated by monitoring the UV–Visible spectrophotometer. The UV–Visible spectra of the synthesized nanosensor exhibited a characteristic absorption band at 400 nm. The SPR band was monitored upon the addition of different pesticides, such as Acetamiprid, Penoxyprop-p-ethyl, Emamictin Benzoate, Paraquat, Thiamethxion, lambda Cyhalothrine, Prochloraz, Acetochlor Chloropyrifos, Pendimethalin and Cypermethrine. Only paraquat considerably affected the UV peak by quenching and shifting in the absorption peak (400–485 nm) with redshift 85 nm (Fig. 4a). Furthermore, the color of Imida-AgNPs was changed from yellow to light reddish, which indicated the strong binding affinity of Paraquat with Imida-AgNPs. Due to its high sensitivity and specificity, the synthesized nanosensors were used for the detection of paraquat in water and soil samples. The detection of pesticides was also checked at different medium in the range of pH (2–14). The results showed that paraquat can be easily detected in the medium with pH range (4–12) but the highly acidic medium (pH < 4) affected the detection (Fig. 4b). Furthermore, the interaction of various concentrations of paraquat with Imida-AgNPs was also studied. The results showed that there was a linear relation between Imida-AgNPs concentration and paraquat (Fig. 4f). The minimum and maximum sensing of paraquat in different solutions were determined by change in color and quenching of the peak. This was done by adding the different concentrations of paraquat in Imida-AgNPs solutions. Upon increasing the concentration above 20 µM, the change in color from yellow to light pink and quenching of SPR band was observed (Fig. 5d). Similarly, the high detection limit was 180 µM (Fig. 4c, d). The strong interaction between imidacloprid and silver ions has been explained by the electron-donating ability of the nitrogen atom of imidacloprid and silver ions [41].

To measure selectivity, different pesticides including Phenoxyprop-p-ethyl, Prochloraz, Acetochlor, Aendimethalin, Cypermethrine, lambda Cyhalothrine, and Emamictin Benzoate, were tested in combination with paraquat. The results showed that the presence of any of the above-mentioned pesticides not interfered with paraquat (Fig. 4e).

Imida-AgNPs were successfully employed as a chemical-sensor for sensitive and robust determination of paraquat in water and soil samples. Different properties of the sensor towards parquet were compared with those of some previously reported sensors for the detection of paraquat (Table 1). The proposed simple and easy method was found to be valuable for the colorimetric detection of pesticides.

Real Sample Analysis

The synthesized nanosensor was added to the standard solution (20–180 µM) of paraquat in tape water. The results showed that the nanosensor was only specific to paraquat and was free from the influence of various other substances present in the tap water (Fig. 5a). Agricultural soil samples were collected from the local agriculture field. The synthesized nanosensor was added to the soil filtrate containing paraquat. The results suggested that the synthesized nanosensor was specific only to paraquat and was

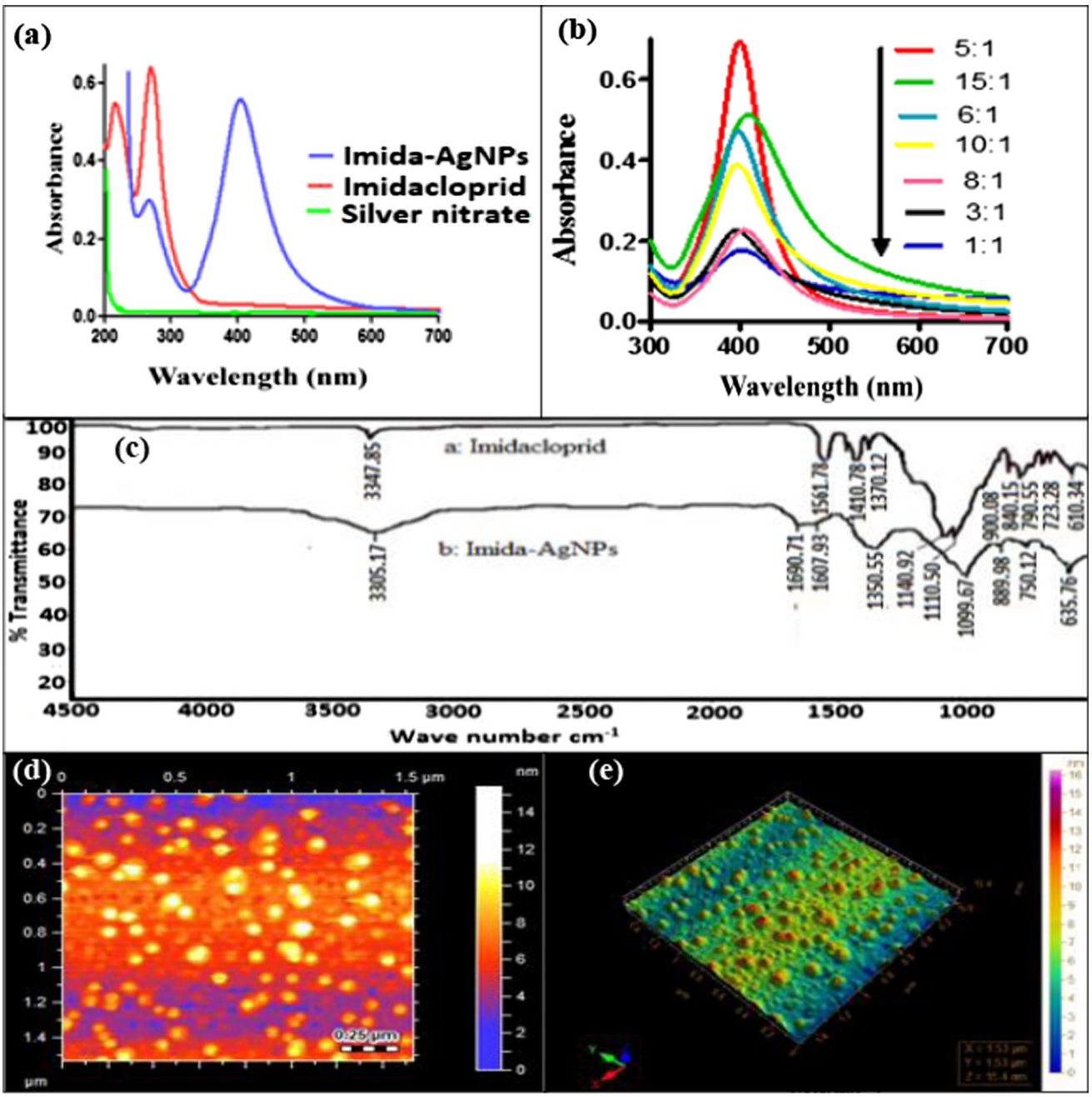

Fig. 2 Characterization of Imid-AgNPs. **a** UV–Visible spectra Imidacloprid, silver nitrate and Imid-AgNPs, **b** UV–Visible spectra Imid-AgNPs synthesized by reacting different ratios of imidacloprid and silver nitrate solution, **c** FT-IR Spectra of both Imidacloprid and Imida-coated AgNPs, **d** and **e** AFM images of Imid-AgNPs

not affected by other substances present in the soil sample (Fig. 5b). Human urine was spiked with a solution (20–180 μM) of paraquat. The synthesized nanosensor was added to the prepared solution. The results suggested that the nanosensor particularly identified paraquat in human urine similar to DI water (Fig. 5c).

Sensing Mechanism

The addition of paraquat to Imida-AgNPs resulted in a change in color from yellow to light reddish. This change was followed by changes in the surface plasmon resonance spectra of the Imida-AgNPs. The paraquat interacted with Imida-AgNPs through the mechanism of π–π stacking of aromatic ring forming charge transfer complexes. In the formation of charge transfer complexes, paraquat with high

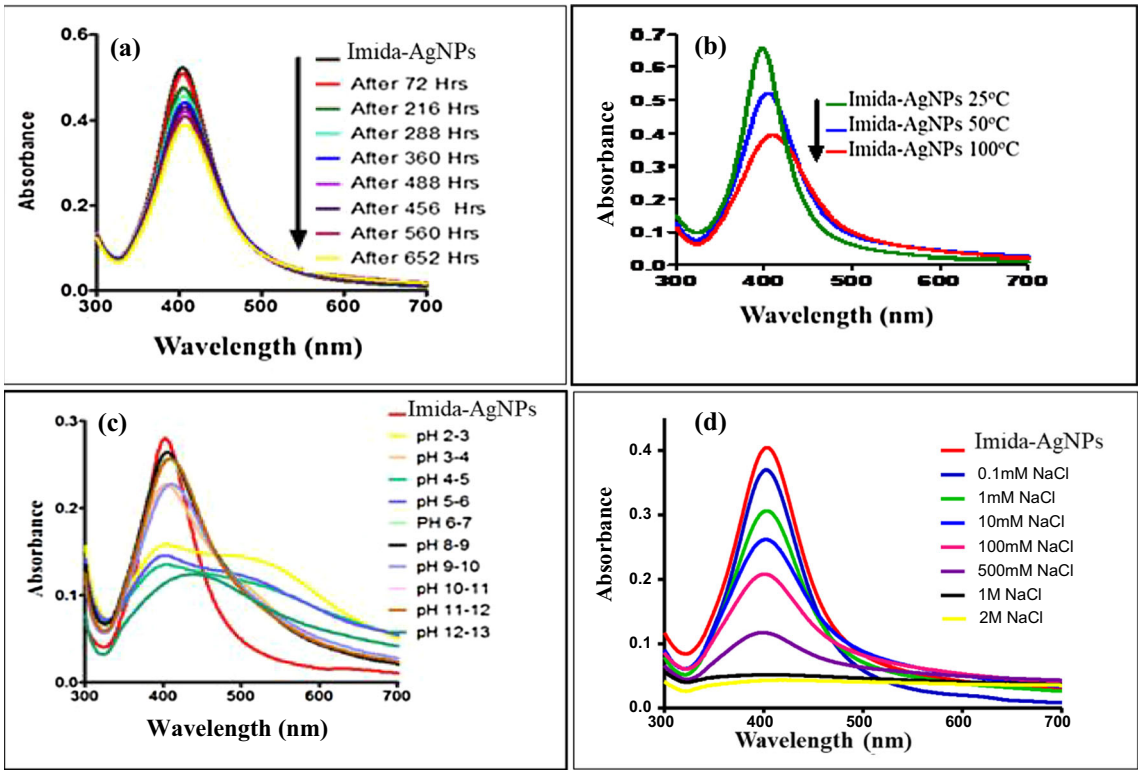

Fig. 3 Stability of Imida-AgNPs. **a** UV–Vis spectra of Imida-AgNPs after different time intervals, **b** effect of temperature on the stability of Imida-AgNPs, **c** effect of pH on stability of Imida-AgNPs and **d** effect of Salt (NaCl) on Stability of Imida-AgNPs

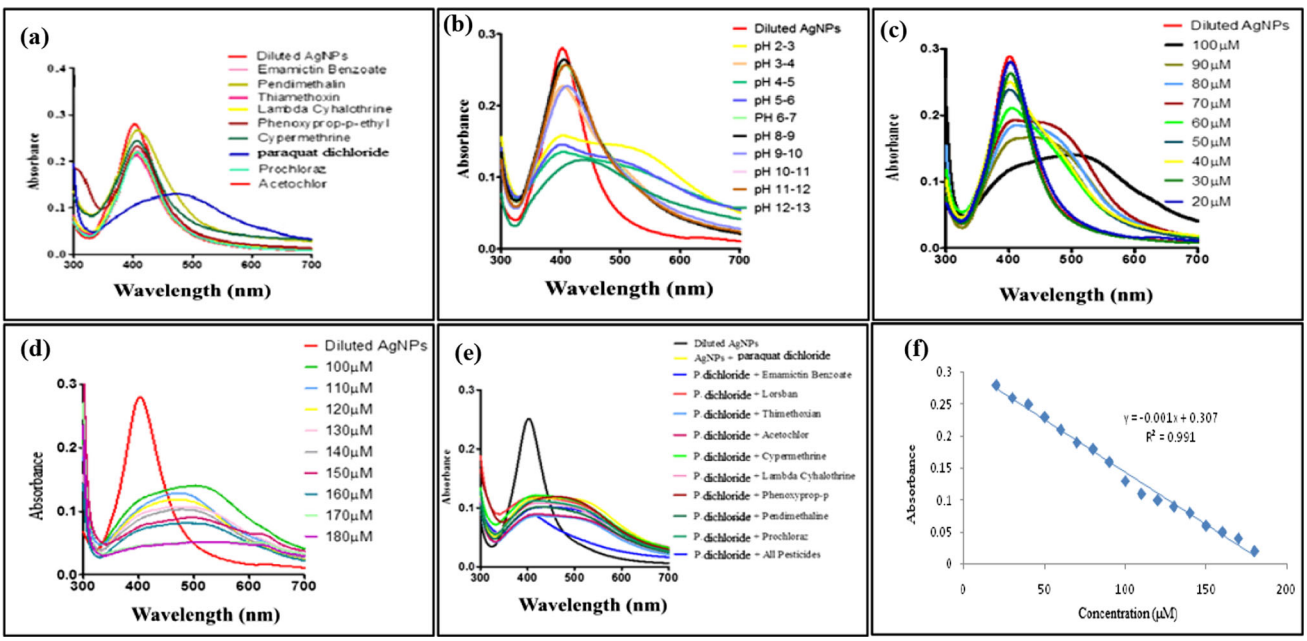

Fig. 4 Detection of Paraquat using Imida-AgNPs. **a** UV–Visible spectra showing the change in SPR peak after addition of available pesticides to Imida-AgNPs, **b** detection of paraquat using Imida-AgNPs in different pH, **c** UV–Vis absorption spectra of Imida-AgNPs by the addition of paraquat in the concentration range of 20–100 µM, **d** UV–Vis absorption spectra of Imida-AgNPs by the addition of paraquat in the concentration range of 100–180 µM and **e** UV–Vis absorption spectra of Imida-AgNPs in the presence of various pesticide (Imidacloprid, acetamiprid, penoxyprop-p-ethyl, emamictin benzoate, cypermethrine, thiamethxion, lambda cyhalothrine, prochloraz, acetochlor chloropyrifos and pendimethalin) and **f** linear regression curve (concentration vs absorbance)

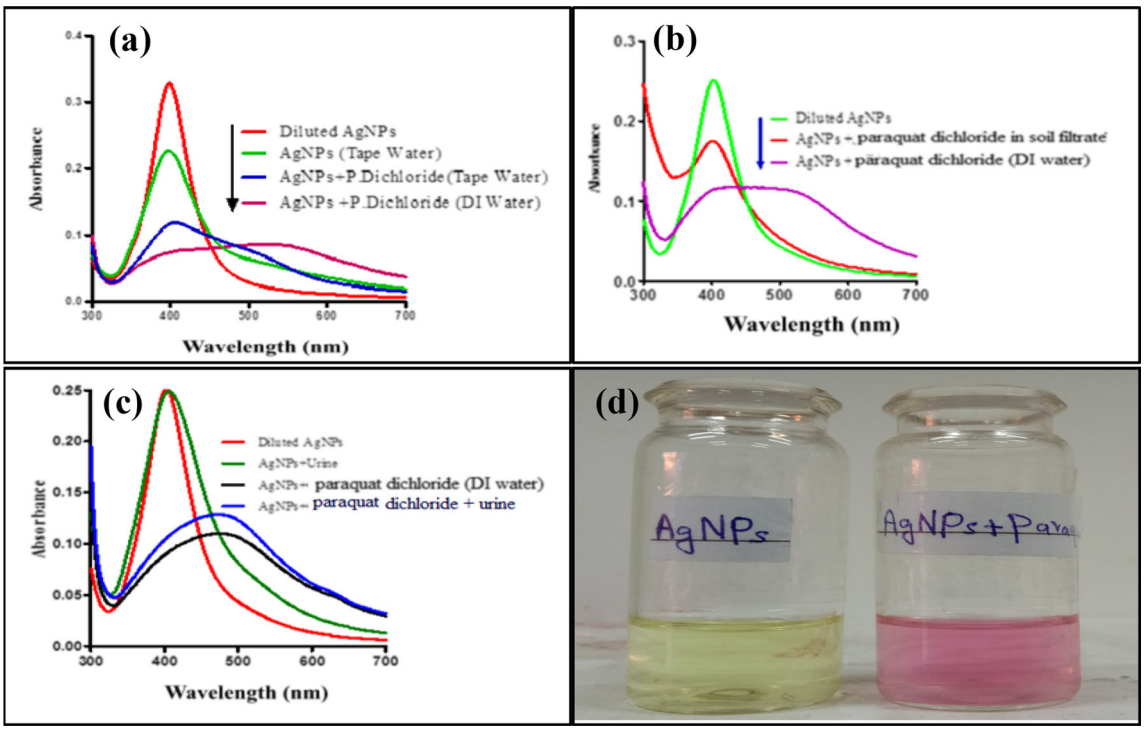

Fig. 5 Detection of paraquat in different samples. **a** Detection of paraquat in tape water using Imida-AgNPs, **b** detection of paraquat soil employing Imida-AgNPs, **c** detection of paraquat in urine sample using Imida-AgNPs and **d** photographs of Imida-AgNPs solution (from yellow to light reddish)

Table 1 Previously reported sensors for the detection of paraquat

Method	Sensor	LOD (μM)	References
Colorimetry	Cyclen dithiocarbamate-functionalized silver nanoparticles	7.21	[42]
Colorimetry	AgNPs Capped with *p* Hydroxybenzoic Acid	8.3	[43]
Fluorescence	Pyrenyl salicylic acid	0.270	[44]
Colorimetry	*Carboxylatopillar[5]arene-Modified Gold Nanoparticles*	0.2	[45]

electronegativity acted as an electron acceptor, and the aromatic ring of imidacloprid (as capping agent of Imida-AgNPs) acted as electron donors. This resulted changes in the surface plasmon resonance spectra [46]. The model of interaction between paraquat and Imida-AgNPs which caused the aggregation is proposed in Fig. 6.

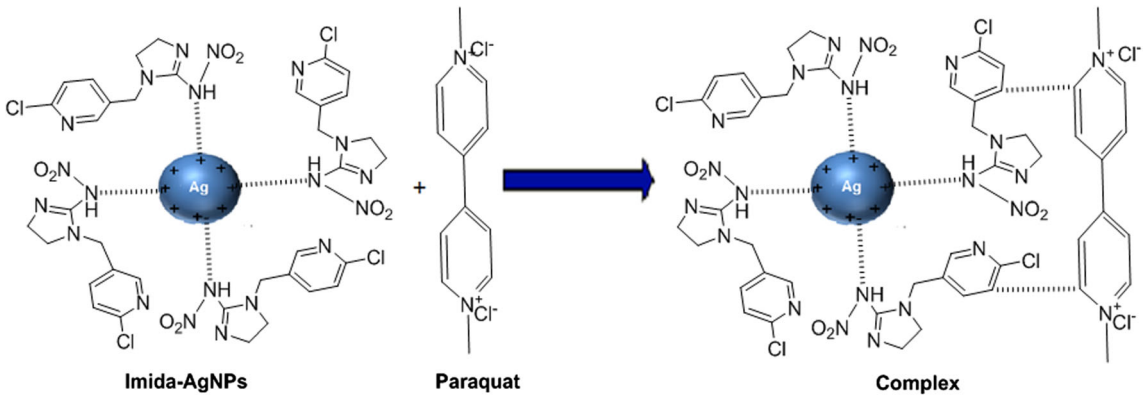

Fig. 6 Sensing mechanism and interaction between paraquat and Imida-AgNPs

Conclusions

Imida-AgNPs were successfully employed as a chemical sensor for sensitive and robust determination of paraquat in environmental and agricultural samples. The synthesized nanoparticles were found very sensitive for the detection of paraquat with limit of detection (LOD) 6.27 μM under the optimized conditions. The proposed method was found to be valuable for the colorimetric detection of pesticides in real water and soil samples. Furthermore, the strategy can be employed for the detection of hazardous substances in agricultural and environmental samples.

Acknowledgements The authors are grateful to HEJ, ICCBS, University of Karachi Pakistan and Department of Chemistry University of Malakand for instrumental availability.

Compliance with ethical standards

Conflict of interest The authors have no conflicts of interest.

References

1. F. Laghrib, M. Bakasse, S. Lahrich, and M. El Mhammedi (2020). *Mater Sci Eng C* **107**, 110349.
2. R. D. Oliveira, J. Duarte, A. S. Navarro, F. Remiao, M. Bastos, and F. Carvalho (2008). *Critic Rev Toxicol* **38**, 13–71.
3. S. Igbedioh (1991). *Arch Environ Health* **46**, 218–224.
4. Z. E. Suntres (2018). *Fitoterapia* **131**, 160–167.
5. T. Kanchan, S. M. Bakkannavar, and P. R. Acharya (2015). *Toxicol Int* **22**, 30.
6. A. Jain, K. K. Verma, and A. Townshend (1993). *Analytica Chimica Acta* **284**, 275–279.
7. S. Wang, L. Zhang, X. Wang, Z. Wang, C. Wen, J. Ma, Z. Gao, and L. Hu (2016). *Int J Clin Exp Med* **9**, 21514–21520.
8. Y. C. Tsao, Y. C. Lai, H. C. Liu, R. H. Liu, and D. L. Lin (2016). *J Anal Toxicol* **40**, 427–436.
9. B. Spangenberg (2012). *JPC* **25**, 262–268.
10. A. P. Vu, T. N. Nguyen, T. T. Do, T. H. Doan, T. H. Ha, T. T. Ta, H. L. Nguyen, P. C. Hauser, T. A. H. Nguyen, and T. D. Mai (2017). *J Chromatogr B* **1060**, 111–117.
11. K. Usui, E. Minami, Y. Fujita, H. Kobayashi, T. Hanazawa, Y. Kamijo, and M. Funayama (2019). *J Pharmacol Toxicol Methods* **100**, 106610.
12. S. Lahrich, H. Hammani, W. Boumya, A. Loudiki, A. Farahi, M. Achak, M. Bakasse, and M. El Mhammedi (2016). *Electroanalysis* **28**, 1012–1022.
13. Z. Zhao, F. Zhang, and Z. Zhang (2018). *Spectrochimica Acta Part A* **199**, 96–101.
14. K. Shrivas, S. Sahu, B. Sahu, R. Kurrey, T. K. Patle, T. Kant, I. Karbhal, M. L. Satnami, M. K. Deb, and K. K. Ghosh (2019). *J Mol Liquids* **275**, 297–303.
15. D. Xiong and H. Li (2008). *Nanotechnology* **19**, 465502.
16. T. M. Tolaymat, A. M. El Badawy, A. Genaidy, K. G. Scheckel, T. P. Luxton, and M. Suidan (2010). *Sci Total Environ* **408**, 999–1006.
17. S. Marin, G. Mihail Vlasceanu, R. Elena Tiplea, I. Raluca Bucur, M. Lemnaru, M. Minodora Marin, and A. Mihai Grumezescu (2015). *Curr Topics Med Chem* **15**, 1596–1604.
18. A. Haider and I. K. Kang (2015). *Adv Mater Sci Eng* **2015**, 165257.
19. S. Ali, A. S. Sharma, W. Ahmad, M. Zareef, M. M. Hassan, A. Viswadevarayalu, T. Jiao, H. Li, and Q. Chen (2020). *Critic Rev Anal Chem* **3**, 1–28.
20. C. Rao, G. Kulkarni, P. J. Thomas, and P. P. Edwards (2002). *Chemistry* **8**, 28–35.
21. S. Bruzzone, M. Malvaldi, G. P. Arrighini, and C. Guidotti (2005). *J Phys Chem B* **109**, 3807–3812.
22. D. Xiong, M. Chen, and H. Li (2008). *Chem Commun* **7**, 880–882.
23. X. H. N. Xu, W. J. Brownlow, S. V. Kyriacou, Q. Wan, and J. J. Viola (2004). *Biochemistry* **43**, 10400–10413.
24. S. J. Huo, X. K. Xue, Q. X. Li, S. F. Xu, and W. B. Cai (2006). *J. Phys. Chem. B* **110**, 25721–25728.
25. L. Hua, J. Chen, L. Ge, and S. N. Tan (2007). *J Nanoparticle Res* **9**, 1133–1138.
26. S. T. Dubas and V. Pimpan (2008). *Talanta* **76**, 29–33.
27. Y. Mishra, S. Mohapatra, D. Kabiraj, B. Mohanta, N. Lalla, J. Pivin, and D. Avasthi (2007). *Scripta Materialia* **56**, 629–632.
28. P. Vasileva, B. Donkova, I. Karadjova, and C. Dushkin (2011). *Colloids Surf A* **382**, 203–210.
29. Y. He, B. Xu, W. Li, and H. Yu (2015). *J Agric Food Chem* **63**, 2930–2934.
30. A. Elbert, B. Becker, J. Hartwig, and C. Erdelen, *Pflanzenschutz-Nachrichten Bayer* (Bayer Print, Leverkusen, 1991).
31. S. O. Duke, J. J. Menn and J. R. Plimmer, ACS Publications, Washington (1993).
32. Z. Rafiq, R. Nazir, M. R. Shah, and S. Ali (2014). *J Environ Chem Eng* **2**, 642–651.
33. M. R. Shah, S. Ali, M. Ateeq, S. Perveen, S. Ahmed, M. F. Bertino, and M. Ali (2014). *New J Chem* **38**, 5633–5640.
34. S. Ali, M. Bacha, M. R. Shah, W. Shah, K. Kubra, A. Khan, M. Ahmad, A. Latif, and M. Ali (2020). *Biotechnol Appl Biochem*. https://doi.org/10.1002/bab.2018.
35. S. Ali, S. Perveen, M. Ali, M. R. Shah, E. Khan, A. S. Sharma, H. Li, and Q. Chen (2019). *J Clust Sci* **31**, 1–11.
36. S. Ali, S. Perveen, M. Ali, T. Jiao, A. S. Sharma, H. Hassan, S. Devaraj, H. Li, and Q. Chen (2020). *Mater Sci Eng C* **108**, 110421.
37. Y. Harada, G. S. Girolami, and R. G. Nuzzo (2004). *Langmuir* **20**, 10878–10888.
38. K. Wagers, T. Chui, and S. Adem (2014). *IOSR J Appl Chem* **7**, 15–20.
39. C. Levard, S. Mitra, T. Yang, A. D. Jew, A. R. Badireddy, G. V. Lowry, and G. E. Brown Jr. (2013). *Environ Sci Technol* **47**, 5738–5745.
40. S. Ali, S. Perveen, M. R. Shah, M. Zareef, M. Arslan, S. Basheer, S. Ullah, and M. Ali (2020). *J Nanoparticle Res* **22**, 1–12.
41. S. F. Yuan, Z. J. Guan, W. D. Liu, and Q. M. Wang (2019). *Nat Commun* **10**, 1–7.
42. J. V. Rohit and S. K. Kailasa (2014). *J Nanoparticle Res* **16**, 2585.
43. G. Gusrizal, S. J. Santosa, E. S. Kunarti, and B. Rusdiarso (2019). *Indonesian J Chem* **2**, 102–111.
44. S. Yuttakovit, T. Santiwat, K. Pratumyot, K. Srikittiwanna, M. Sukwattanasinitt, and N. Niamnont (2020). *J Photochem Photobiol A* **397**, 112570.
45. H. Li, D. X. Chen, Y. L. Sun, Y. B. Zheng, L. L. Tan, P. S. Weiss, and Y. W. Yang (2013). *J Am Chem Soc* **135**, 1570–1576.
46. G. Gusrizal, S. J. Santosa, E. S. Kunarti, and B. Rusdiarso (2020). *Indonesian J Chem* **20**, 688–696.